Available online at www.sciencedirect.com
SCIENCE DIRECT®
Colloids and Surfaces B: Biointerfaces 41 (2005) 285–298
COLLOIDS AND SURFACES B
www.elsevier.com/locate/colsurfb

Properties of two-component Langmuir monolayer of single chain perfluorinated carboxylic acids with dipalmitoylphosphatidylcholine (DPPC)

Hiromichi Nakahara [a], Shohei Nakamura [a], Hideya Kawasaki [b], Osamu Shibata [a,*]

[a] *Division of Biointerfacial Science, Graduate School of Pharmaceutical Sciences, Kyushu University, 3-1-1 Maidashi, Higashi-ku, Fukuoka 812-8582, Japan*
[b] *Department of Chemistry, Graduate School of Science, Kyushu University, 6-1-1 Hakozaki, Higashi-ku, Fukuoka 812-8581, Japan*

Received 13 April 2004; accepted 25 June 2004

Abstract

The surface pressure (π)– and the surface potential (ΔV)–area (A) isotherms were obtained for two-component monolayers of four different perfluorocarboxylic acids (FC*n*s; perfluorododecanoic acid: FC12, perfluorotetradecanoic acid: FC14, perfluorohexadecanoic acid: FC16, perfluorooctadecanoic acid: FC18) with dipalmitoylphosphatidylcholine (DPPC) on substrate solution of 0.15 M NaCl (pH 2.0) at 298.2 K as a function of compositions in the mixtures by employing the Wilhelmy method, the ionizing electrode method, the fluorescence microscopy, and the atomic force microscopy. The data for the two-component monolayers on these systems were analyzed in terms of the additivity rule. Assuming a regular surface mixture, the Joos equation which allows one to describe the collapse pressure of a two-component monolayer with miscible components was used to declare the miscibility of the monolayer state, and an interaction parameter and an interaction energy were calculated. The new finding was that FC*n*s and DPPC are miscible or immiscible depending on chain length increment of fluorocarbon part. That is, FC12/DPPC monolayer was perfectly miscible, and FC14/DPPC, and FC16/DPPC ($0 \leq X_{FC16} \leq 0.3$) monolayers were partially miscible. While FC16/DPPC ($0.3 < X_{FC16} < 1$) and FC18/DPPC systems are immiscible in the monolayer state. Furthermore, the mean molecular area, the surface dipole moment, and the phase diagrams enabled us to estimate the molecular orientation of four different perfluorocarboxylic acids/DPPC in the two-component monolayer state. One type of phase diagrams was obtained and classified into the positive azeotropic type. The miscibility of FC*n*s and DPPC in the monolayer was also supported by fluorescence microscopy and atomic force microscopy. FC12/DPPC, FC14/DPPC and FC16/DPPC ($0 \leq X_{FC16} \leq 0.3$) two-component monolayers on 0.15 M NaCl (pH 2) showed that FC12, FC14 and FC16 ($0 \leq X_{FC16} \leq 0.3$) can dissolve or partially dissolve the ordered solid DPPC domains formed upon compression. This indicates that these fluorinated amphiphiles soften or harden the lipid depending on their chain length.

Keywords: Langmuir monolayer; Perfluorocarboxylic acid; Dipalmitoylphosphatidylcholine (DPPC); Surface potential; Two-dimensional phase diagram; π–A isotherm; ΔV–A isotherm; Fluorescence microscopy; Atomic force microscopy

1. Introduction

Fluorocarbons are characterized by their exceptional chemical and biological inertness, extreme hydrophobicity, lipophobicity, high gas-dissolving capacity, low surface tension, high fluidity and spreading coefficients, high density, absence of protons, and magnetic susceptibility. These unique properties are the foundation for a wide range of biomedical applications. An injectable fluorocarbon-in-water emulsion is in advanced clinical trials as a temporary oxygen carrier (blood substitute) to prevent the surgical and critical care patient tissue from hypoxia or ischemia. A liquid fluorocarbon is in phase II/III clinical trials for treatment of acute respiratory failure through liquid ventilation. Several fluorocarbon-based contrast agents for ultrasound imaging are in various stages of clinical investigation. Multiple families of well-defined

* Corresponding author. Tel.: +81 92 642 6669; fax: +81 92 642 6669.
E-mail address: shibata@phar.kyushu-u.ac.jp (O. Shibata).
URL: http://kaimen.phar.kyushu-u.ac.jp/ (O. Shibata).

0927-7765/$ – see front matter © 2004 Elsevier B.V. All rights reserved.
doi:10.1016/j.colsurfb.2004.06.013

pure fluorinated surfactants have recently been synthesized [1–6]. These surfactants have a modular structure which allows stepwise adjustment of their physicochemical characteristics. Their polar head group is derived from polyols, sugars, aminoacids, amides, amine oxides, phosphocholine, phosphatidylcholine, etc. Fluorinated surfactants are much more surface active than their corresponding hydrocarbon analogues, and they display a greater tendency to assemble, thus forming well-ordered and stable supramolecular assemblies such as vesicles, tubules, fibers, ribbons, etc. Fluorinated amphiphiles also form a variety of stable reverse and multiple emulsions and gels. These systems are being investigated as drug delivery devices [7–12].

Various kinds of two-component hydrocarbon monolayers spread at air/water interface have been extensively studied by many investigators [13–16]. Considering the importance of fluorinated amphiphiles in advanced clinical trials [1–6], it is necessary to know the way how these fluorinated materials interact with their environment. In this respect, the two-component monolayers work as a model system in advanced clinical trials. Although perfluorocarboxylic acids have toxicity, as long as we know, the systematic study for the two-component monolayers of perfluorocarboxylic acids/DPPC has not been reported yet except for partially fluorinated carboxylic acids [17–20]. The presence of additivity for surface potential values of the mixtures or its good linearity against the composition suggests the absence of any particular interactions between the monolayer components. The surface potential has been proved to be more sensitive at earlier stages of compression compared with surface pressure.

The authors have studied the two-component system of a phospholipid (dipalmitoylphosphatidylcholine, DPPC) with hydrocarbon as well as fluorocarbon fatty acids and reported that in the two-dimensional phase or monolayer film phase, the fluorocarbon acids can form a two-component monolayer with DPPC accompanied by a rather strong intermolecular interaction. This suggests that the head groups' interaction also contributes more to structure formation than hydrophobic interaction [21]. In the previous study, however, the systems were restricted only to the mixtures of single chain perfluorocarboxylic acids (perfluorodecanoic acid and perfluorooctadecanoic acid) and DPPC by π–A and ΔV–A isotherms measurements. The good miscibility for the above systems may be attributed only to the interaction between the head groups. In order to obtain more systematic generalized information concerning the two-dimensional molecular interaction between fluorocarbon and hydrocarbon chains at the air/water interface, we investigated in this paper the two-component monolayer behaviors of perfluorocarboxylic acids/DPPC system also supporting by fluorescence microscopy and atomic force microscopy.

The phase behaviors in the two-component monolayer states will be examined from a view point of the additivity rule for the mean molecular surface area, the surface potential, and the surface dipole moment, referring the phase diagrams in the previous studies [22–24]. Further, the π–A and ΔV–A (or $\mu_{\perp}$–A) relations will allow us to estimate the molecular orientation of perfluorocarboxylic acids/DPPC in their two-component monolayer states. In addition, the monolayers were examined by fluorescence microscopy and atomic force microscopy.

2. Experimental

Perfluorocarboxylic acids [perfluorododecanoic (FC12), perfluorotetradecanoic (FC14), perfluorohexadecanoic (FC16) and perfluorooctadecanoic acids (FC18)] were purchased from Fluorochem (United Kingdom). They were purified by repeated recrystallizations from *n*-hexane/acetone mixed solvent (11:1, v/v). The purity of these amphiphiles was checked by ^{19}F NMR measurement (UNITY INOVA 400Spectrometer, Varian, USA) and by elemental analysis; the observed and calculated values were in satisfactory agreement (<±0.3%). Dipalmitoylphosphatidylcholine (L-α-1-palmitoyl-2-hydroxy-*sn*-glycero-3-phosphocholine: DPPC) was purchased from Avanti Polar Lipids Inc. (Birmingham, Alabama, USA) and was used without further purification. The purity of DPPC was checked by TLC which showed one spot. Stock solutions of FC*n*s or DPPC (1.35 mM) were prepared in *n*-hexane/ethanol mixture (9/1 in v/v, the former from Merck, Uvasol, and the latter from Nacalai Tesque), and 50 μl of its solution with different molar ratios was spread at the air/aqueous solution interface.

The substrate solution of 0.15 M (1 M = 1 mol dm^{-3}) sodium chloride (Nacalai Tesque) was prepared using thrice distilled water (surface tension, 71.96 mN m^{-1} at 298.2 ± 0.1 K; resistivity, 18 MΩ cm), where pH of the solution was maintained at 2 by hydrochloric acid (ultra fine grade; Nacalai Tesque). Sodium chloride was roasted at 973 K for 24 h to remove any surface active organic impurity. The surface pressure of the monolayer was measured using an automated home-made Wilhelmy film balance, which was the same as that used in the previous studies [23,24]. The surface pressure balance (Mettler Toledo, AG245) had resolution of 0.01 mN m^{-1}. The surface measuring system was equipped with the filter paper (Whatman 541, periphery 4 cm). The trough was made from a 750 cm^2 Teflon-coated brass. The π–A isotherms were recorded at 298.2 ± 0.1 K. The monolayer was compressed at the speed of 0.103 nm^2 molecule^{-1} min^{-1}, because no influence of difference in the compression rate (at 0.066, 0.103 and 0.200 nm^2 molecule^{-1} min^{-1}) could be detected within the limits of the experimental error.

Surface potential was also recorded while the monolayer was compressed. It was monitored using an ionizing ^{241}Am electrode at 1–2 mm above the interface, while a reference electrode dipped in the subphase. The standard deviations for area and surface potential measurements were ∼0.01 nm^2 and ∼5 mV, respectively. Other experimental conditions were the same as described in the previous papers [21–24,27].

2.1. Fluorescence microscopy

Fluorescence image was observed using an automated home-made Wilhelmy film balance (Mettler Toledo, AG245; resolution 0.01 mN m^{-1}) equipped with a BM-1000 fluorescence microscope (U.S.I. System) [23,24]. Surface pressure and fluorescence microscopy images were recorded simultaneously upon compression. The fluorescent probe (1 mol%) was 3,6-bis(diethylamino)-9-(2-octadecylcarbonyl)phenyl chloride (R18, Molecular Probes). A 300 W xenon lamp (XL 300, Pneum) was used for fluorescence excitation. Excitation and emission wavelengths were selected by an appropriate beam splitter/filter combination (Mitutoyo band path filter 546 nm, cut filter Olympus 590 nm). The monolayer was observed using 20-fold magnification and long-distance objective lens (Mitutoyo f = 200/focal length 20 mm). Micrographs were recorded with a video camera (757 JAI ICCD camera, Denmark) connected to the microscope, directly into computer memory via an online image processor (Vaio PCV-R53 Sony: Video Capture Soft). The entire optical set-up was placed on an active vibration isolation unit (Model-AY-1812, Visolator, Japan). All measurements were performed at 298.2 ± 0.1 K. Image analysis was performed using NIH image (developed at the US National Institutes Health). All images presented appear as taped without image enhancement.

2.2. Atomic force microscopy and dynamic force microscopy

AFM images were captured with SPA 400 (Seiko Instruments Co., Japan) under the normal atmosphere, using silicon tips with a spring constant of 17 N m^{-1} (Olympus Co., Japan) [25]. The microscope was operated in the dynamic force mode (DFM) and the phase contrast mode at resonance frequencies of 120–140 kHz [26]. The cantilever was forced to oscillate near its resonance frequency. Muscovite mica was glued to microscope slides with low melting temperature epoxy glue and then freshly cleaved with adhesive tape in a laminar flow. LB-film preparations were carried out with a home-made LB trough. Freshly cleaved mica was used as a supporting solid substrate for the film deposition. At 20 mN m^{-1}, transfer velocity of 10 mm min^{-1} was used for film forming materials on 0.15 M NaCl (pH 2) containing subphase. AFM images were performed for LB films at 298.2 ± 2 K.

3. Results and discussion

3.1. Surface pressure–, surface potential– and dipole moment–area isotherms

Since the monolayer of the shorter chain FC12 was found to be unstable on a pure water substrate, the substrate condition was examined first. The optimum pH of the substrate was found to be less than 2.0 under the condition of 0.15 M NaCl. So pH 2 was kept throughout the experiments in order to avoid dissolution of the film-forming materials toward the subphase.

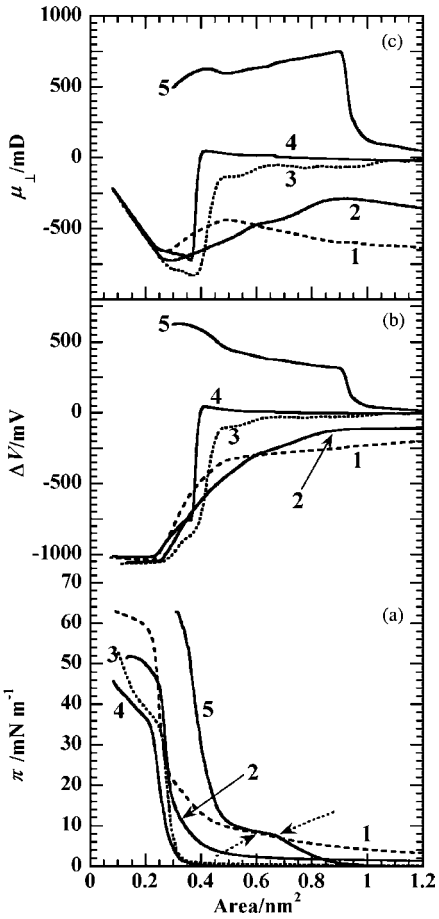

Fig. 1. Surface pressure (π)–area (A) isotherms (a), surface potential (ΔV)–A isotherms (b), and surface dipole moment ($\mu_\perp$)–A isotherms (c) of FC12: (1: dashed line), FC14: (2), FC16: (3: dotted line), FC18: (4) and dipalmitoylphosphatidylcholine (DPPC: 5) pure systems on 0.15 M NaCl (pH 2) at 298.2 K.

The π–A, ΔV–A and $\mu_\perp$–A isotherms obtained for pure FCn (n = 12,14, 16 and 18), and DPPC at 298.2 K on 0.15 M sodium chloride (pH 2) solution are shown in Fig. 1. The monolayer of FC12 is stable up to 59 mN m^{-1} with a transition from a disordered to a ordered state at 8.2 mN m^{-1} and 0.61 nm^2 as described previously [27]. While the monolayers of FC14, FC16 and FC18 are collapsing from an ordered state at 45, 35 and 35 mN m^{-1}, respectively. All extrapolated areas of FCns in the ordered state are concentrated at approximately 0.30 nm^2, which is in agreement with that in previous papers [27,28]. This value indicates that the fluorinated chains are in closely contact at high surface pressure.

Both π–A and ΔV–A isotherms of DPPC monolayer at the surface of 0.15 M NaCl (pH 2) solution (Fig. 1) is very close to those previously reported [29–31], except for minor distinctions caused by dissimilarities in subphase composition. Detectable π value appears near A = 0.67 nm^2,

reflecting the formation of continuous liquid expanded (LE) phase. The plateau of π at ~7.6 mN m^{-1} represents the liquid expanded–liquid condensed (LE–LC) coexistence region, and further sharp increase in π corresponds to the formation of a compact LC phase. Evolution of the (ΔV–A) isotherm reflects that of π–A isotherm; at $A > 0.8$ nm^2 the ΔV values are not reproducible, because the monolayer likely consists of large domains of LE and rarefied gas phases.

The surface potentials of FCn (n = 12, 14, 16 and 18) are always negative and reach values of ca. −1000 mV at the collapse pressures. This results from the strong electronegative fluorine atoms [32–34]. On the contrary, that of DPPC is positive and changes from 0 to ca. 620 mV.

The important feature of the surface potential is that it allows the Langmuir monolayer to be probed at much earlier stages of monolayer compression in comparison with surface–pressure isotherms [29,35,36]. Such behavior is more clear in the case of DPPC. The appearance of a critical area at which the surface potential rises sharply is also worth mentioning, as it indicates the structuring of monolayer as is detected by a number of other experimental techniques [37–45]. Though the idea of a critical packing density was suggested about 10 years ago [46], it has been mostly overlooked in the study of Langmuir monolayers. Iwamoto and his coworkers do mention [47–49] a critical area in the recent papers, but with a different definition from that employed here. They include a theoretical approach for the phase transition of molecular orientation, while the calculated value for the critical area of long-chain aliphatic compounds is not consistent with surface potential experiment.

The results of the surface dipole moment for close-packed monolayers at a surface pressure up to 30 mN m^{-1} are shown in Fig. 1, where dependence of dipole moment ($\mu_\perp$) on the polar head group is clearly demonstrated. That is, looking at the FCn (n = 12, 14, 16 and 18), the surface dipole moment ($\mu_\perp$) decreases from vicinity of −700 mD to around −660 mD via small hump for FC12, from −350 mD to −710 mD for FC14, from ca. 0 mD to −740 mD for FC16 and from 0 mD to −640 mD for FC18 with decreasing the surface area, respectively. Judging from sharp negative jumps of the $\mu_\perp$–A isotherms for FC16 and FC18, it became clear that the orientation of these molecules is sharply changed at mean surface area around 0.40–0.45 nm^2. On the contrary, DPPC shows the change from 40 mD to 650 mD showing the sharp positive jump.

3.2. Ideality of mixing

Turning to the discussion toward the two-component systems, the monolayer system composed of the single-chain perfluorocarboxylic acids (FCns) with DPPC has been studied in order to clarify the effect of molecular structures on the interaction, the miscibility, and the monolayer state. For the above purpose, the π–A, ΔV–A and $\mu_\perp$–A isotherms of two-component monolayers of DPPC and FCn (n = 12, 14, 16 and 18) were therefore measured for various mole fractions of $X_{\mathrm{FC}n}$ at 298.2 K on 0.15 M NaCl (pH 2) in Fig. 2.

3.2.1. FC12, FC14, FC16 and FC18/DPPC two-component system

For FC12/DPPC, FC14/DPPC, FC16/DPPC and FC18/DPPC two-component system in Fig. 2, the π–A, ΔV–A and $\mu_\perp$–A isotherms of seven discrete mole fractions are also inserted in the same figures. For the π–A isotherms at the surface pressure higher than 25 mN m^{-1}, all the curves of the two-component systems exist between those of the respective pure components, and they successively increased with the mole fraction of individual FCn. As for FC12/DPPC two-component system, the π–A isotherm displays a phase transition pressure that increases with X_{FC12} and with DPPC content at the both sides in Fig. 3. This behavior is a first evidence of the miscibility of the two components within the binary monolayer. As it is difficult to ascertain the transition pressure values on π–A isotherms for a certain mole fraction, we have examined two-component monolayers by fluorescence microscopy (later section).

The interaction between FC12, or FC14, or FC16 or FC18 and DPPC molecules was investigated by examining whether the variation of the mean molecular areas as a function of $X_{\mathrm{FC}n}$ satisfies the additivity rule [50]. Comparison between the experimental mean molecular areas and the mean molecular areas calculated for ideal mixing is shown in Fig. 4 for four surface pressures (5, 15, 25 and 35 mN m^{-1}). For π = 5 mN m^{-1}, FC12/DPPC system (Fig. 4a) shows a large negative deviation from the theoretical line, indicating attractive interaction between FC12 and DPPC. This may result from the fact that at such low surface pressures the interactions between DPPC and FC12 (both in the disordered state) are mainly governed by the attractions between the polar heads. For π = 15 mN m^{-1}, a positive deviations are observed, reflecting the coexistence region of both components of FC12 and DPPC. But at $\pi > 25$ mN m^{-1}, the variation almost follows the additivity rule. This indicates that FC12 and DPPC are almost ideally mixed in the monolayer. Even though FC12 has shorter chain length than DPPC, attractive interaction between FC12 and DPPC head groups is maximized and compensated by repulsion between the fluorocarbon segment and the DPPC chain.

The influence of X_{FC12} on the ΔV–A and $\mu_\perp$–A isotherms is shown in Fig. 2a. Both the surface potential (ΔV) and the surface dipole moment ($\mu_\perp$) of the monolayer clearly indicate that all the curves of the two-component systems exist between those of the respective pure components, and they successively change with the mole fraction at the area less than 0.80 nm^2. That is, if the collapse pressure is higher, the lager values of ΔV and $\mu_\perp$ are demonstrated.

Analysis of ΔV for the two-component monolayer in terms of the additivity rule is presented in Fig. 5. For FC12/DPPC at π = 5 mN m^{-1}, Fig. 5a shows a sigmoid deviation from the rule, indicating the effect of LE state of DPPC and the disordered state of FC12. For the other pressures, comparison of

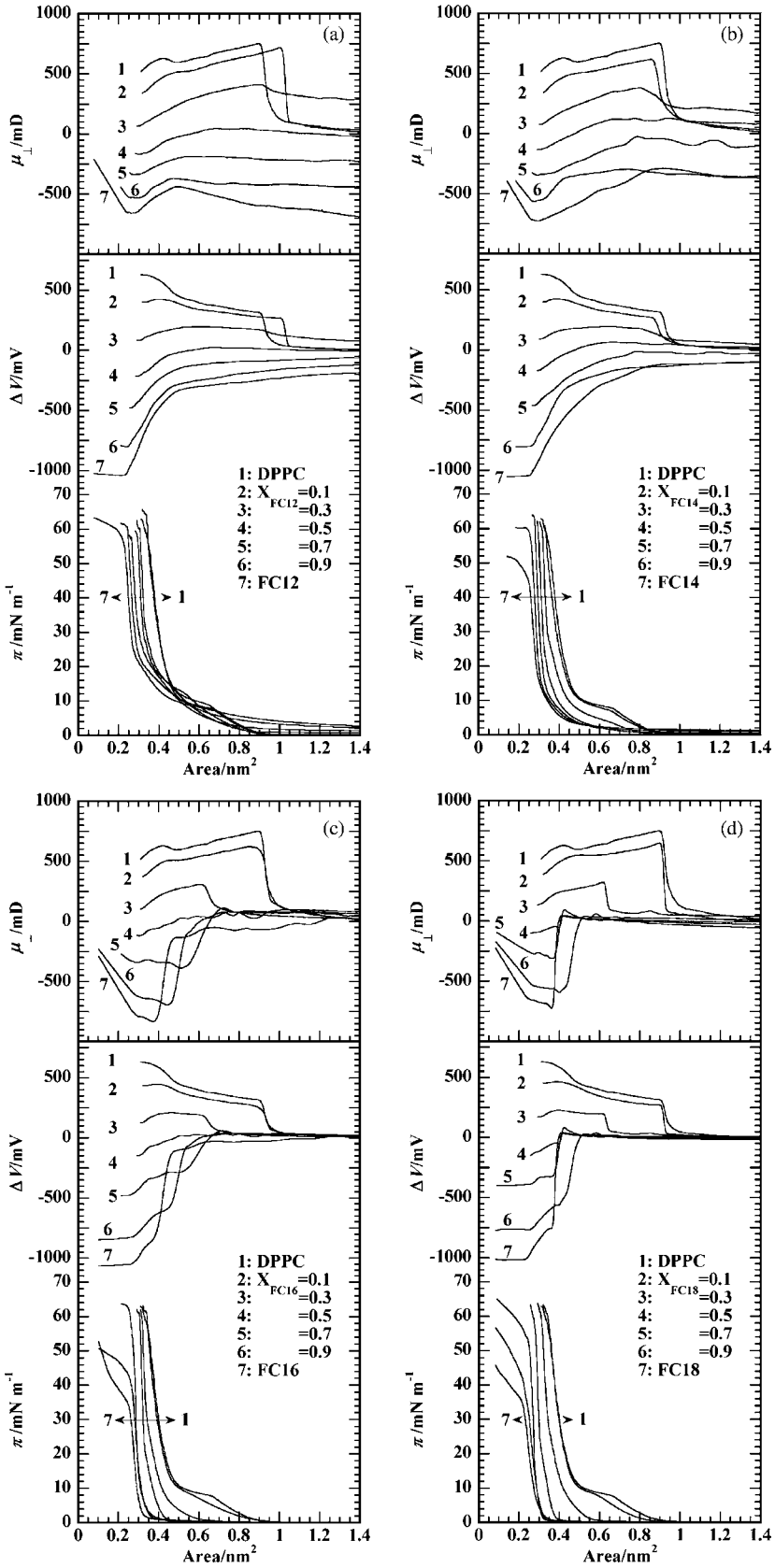

Fig. 2. Two-component monolayer system; surface pressure (π)–area (A) isotherms, surface potential (ΔV)–A isotherms, and surface dipole moment ($\mu_\perp$)–A isotherms of FC12, FC14, FC16 and FC18 with DPPC as a function of FCn mole fraction on 0.15 M NaCl (pH 2) at 298.2 K.

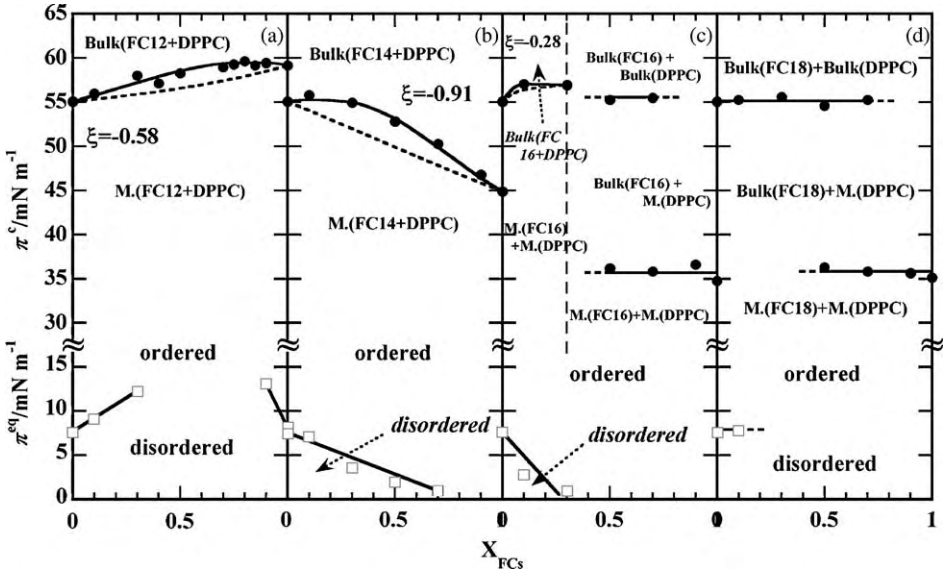

Fig. 3. Variation of the transition pressure (π^{eq}) and the collapse pressure (π^{c}) as a function of X_{FCns} on 0.15 M NaCl (pH 2) at 298.2 K. The dashed line was calculated according to Eq. (1) for $\xi = 0$. (a) FC12/DPPC, (b) FC14/DPPC, (c) FC16/DPPC and (d) FC18/DPPC.

the experimental data with calculated values clearly indicates a good agreement at all surface pressures over X_{FC12} range from 0 to 0.5. At 35 mN m^{-1} for high mole fraction of FC12, the ΔV–X_{FC12} shows a positive deviation which results from the decrement in a tilt angle of the palmitic chain of DPPC by increasing FC12 amount. In the monolayer, DPPC has a minimum molecular area of about 0.46 nm^2 [51,52], which is limited by a cross-section area of the relatively large head

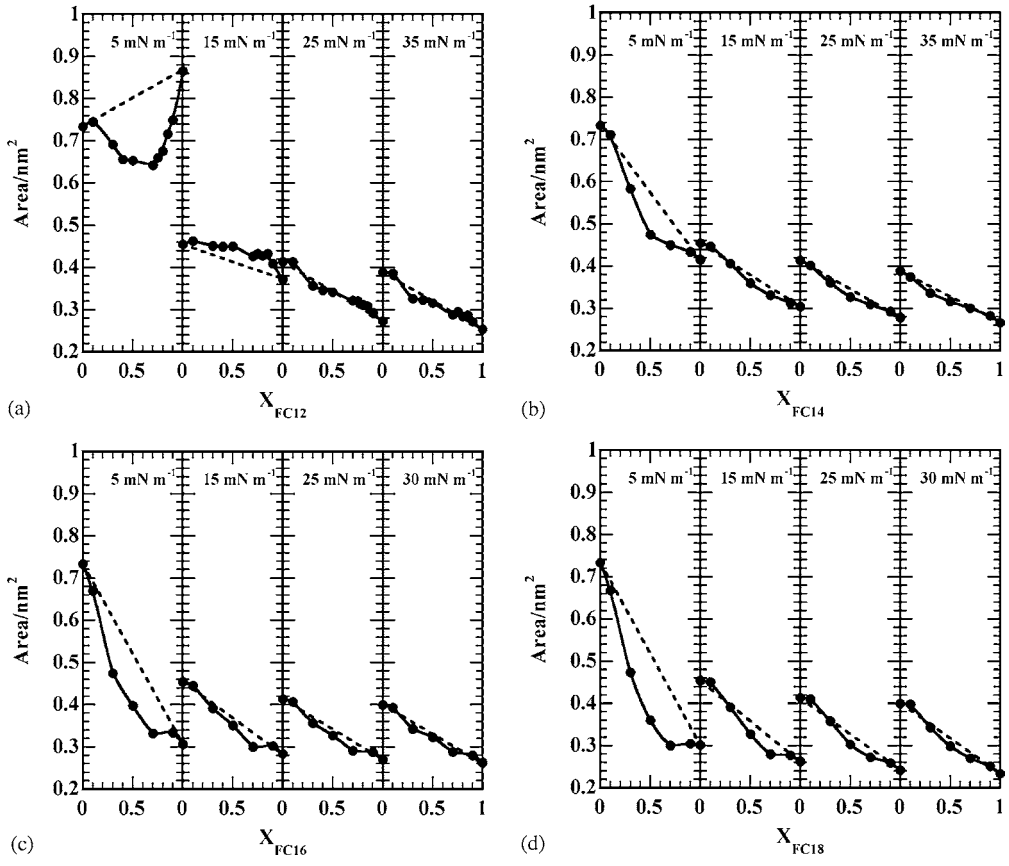

Fig. 4. Mean molecular area (A) of the FCns/DPPC mixed systems as a function of X_{FCns} at four different pressures. The dashed lines were calculated by assuming the additivity rule; the solid points represent experimental values. (a) FC12/DPPC, (b) FC14/DPPC, (c) FC16/DPPC and (d) FC18/DPPC. In (c) and (d), the FC16/DPPC and FC18/DPPC mixed systems are at 30 mN m^{-1}.

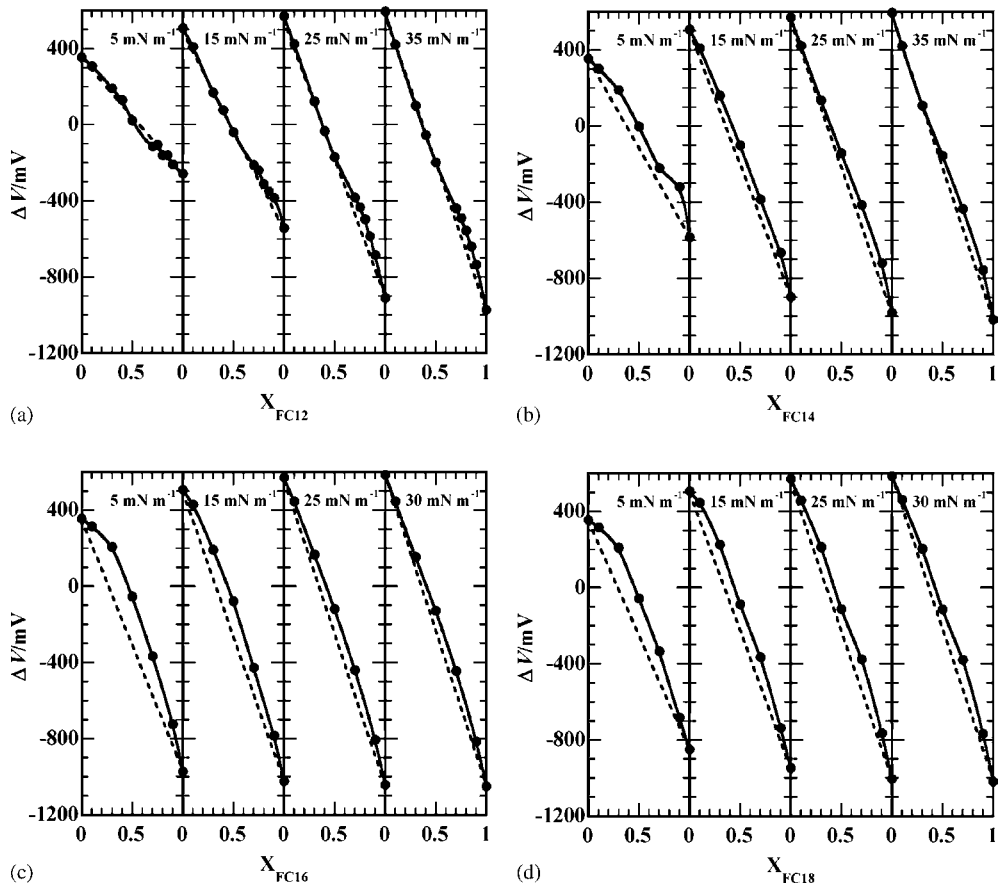

Fig. 5. Surface potential (ΔV) of the FC*n*s/DPPC mixed systems as a function of X_{FCns} at four different pressures. The dashed lines were calculated by assuming the additivity rule. The solid points represent experimental values. (a) FC12/DPPC, (b) FC14/DPPC, (c) FC16/DPPC and (d) FC18/DPPC. In (c) and (d), the FC16/DPPC and FC18/DPPC mixed systems are at 30 mN m^{-1}.

group. The cross-sectional area of an optimally packed, all *trans*, hydrocarbon chain is about 0.20 nm^2 [53], so the hydrocarbon portion of the DPPC molecule would occupy the surface area $A = 2\,\text{nm} \times 0.20\,\text{nm} = 0.40\,\text{nm}^2$ at least. This mismatch results in a tilt angle of the aliphatic chains of 25°–30° and a corresponding reduction in the attractive interactions between the chains [51,54]. The tilting is also accompanied by a decrease in the coherence length of the molecular packing, which is indicative of reduced order in the monolayer state. But increasing the amount of FC12 (X_{FC12} from 0.5 to 1), the hydrocarbon portion of the DPPC molecule would fill with perfluorinated chain. At this composition, we also find closest packing of the aliphatic chains normal to the surface. As the result, ΔV of positive character of DPPC is reflected on the surface potential behavior, and ΔV shows positive deviation from the ideal line.

The above procedures were performed for other perfluorocarboxylic acids/DPPC systems. Other system are very close to this trend, except for minor distinctions caused by dissimilarities in the chain length of perfluorocarboxylic acids. The profile of deviation was similar at four surface pressures (5, 15, 25 and 35 mN m^{-1}), which suggested that the two-component conformation is almost the same. From the π–A isotherms for perfluorocarboxylic acid/DPPC systems, two-dimensional phase diagrams of these systems were constructed by changes of the transition pressure and collapse pressure as a function of mole fraction of FC*n*s. Representative phase diagrams at 298.2 K are shown in Fig. 3.

3.3. Two-dimensional phase diagrams

On the binary systems of FC12/DPPC, FC14/DPPC and FC16/DPPC, the transition pressures from disordered (gaseous or liquid-expanded) to ordered (liquid-condensed) phase are plotted against a mole fraction of FC*n* in Fig. 3. For the FC12/DPPC system, the transition pressures show a positive convex, because both pure two components have a transition pressure. Two components of all other mole fraction may be miscible each other judging from the change of the transition pressure and the collapse pressure in the Fig. 3a. For X_{FC12} lower than 0.3, and 0.9 to 1, π–A isotherm displays a phase transition pressure (π^{eq}) that increases almost linearly with X_{FC12} for the former mole fraction. This behavior is a first evidence of the miscibility of the two components within the mixed monolayer. This can be explained by the fact that film forming molecules become more dense by compression, decrease the surface tension more by the film forming molecule. Then the resultant surface pres-

sure increased. Increase in the transition pressure with mole fraction of FCn means that transition dose appear when the film forming molecules become more dense with the mole fraction. These phenomena resemble the elevation of boiling point and the depression of freezing point in the mixed solution.

On the contrary, for FC14/DPPC and FC16/DPPC, the transition pressure decreases with increasing mole fraction of perfluorocarboxylic acids. This behavior is an indication of the partial miscibility of the two components within the mixed monolayer. From the microscopic point of view, DPPC was compressed by the effect of extremely hydrophobic and lipophobic properties of perfluorocarbon chains, so the resultant transition surface pressure decreased with the mole fraction. In Fig. 3, the two-dimensional phase diagrams of the binary FC14/DPPC, and FC16/DPPC and FC18/DDPC systems also are shown. In the figures, 'M' indicates a two-component monolayer formed by FC*n*s, and DPPC species, while 'Bulk' denotes a solid phase of FC*n*s and DPPC ("bulk phase" may be called "solid phase"). The collapse pressure π^c determined at each mole fraction is indicated by filled circles, where the dotted line shows that the interaction parameter (ξ) is zero.

The coexistence phase boundary between the ordered monolayer phase and the bulk phase can be theoretically simulated by the Joos equation [55]:

$$1 = x_1^s \gamma^1 \exp\left\{\frac{(\pi_m^c - \pi_1^c)w_1}{kT}\right\} \exp\{\xi(x_2^s)^2\} + x_2^s \gamma^2 \exp\left\{\frac{(\pi_m^c - \pi_2^c)w_2}{kT}\right\} \exp\{\xi(x_1^s)^2\} \quad (1)$$

where x_1^s and x_2^s denote the mole fraction in the two-component monolayer of components 1 and 2, respectively, and π_1^c and π_2^c are the corresponding collapse pressures of components 1 and 2. π_m^c is the collapse pressure of the two-component monolayer at given composition of x_1^s and x_2^s. w_1 and w_2 are the corresponding limiting molecular surface area at the collapse points. γ^1 and γ^2 are surface activity coefficients at the collapse point, ξ is the interaction parameter, and kT is the product of the Boltzmann constant and the Kelvin temperature. The solid curve by adjusting the interaction parameter in above equation coincides with the experimental values. FC12/DPPC two-component system has one interaction parameters ($\xi = -0.58$) over the whole mole fraction. The negative interaction parameter implies that the interchange energy between the two different molecules is higher than mean energy of those for the same molecules. And its interaction energies ($-\Delta\varepsilon = \xi\, RT/6$) were calculated to be 240 J mol^{-1} ($\xi = -0.58$). FC14/DPPC system also produced a negative interaction parameter ($\xi = -0.91$ and 376 J mol^{-1}), where the fluorescence microscopy observation showed also homogeneous pattern (the data is not shown). That is, they are partially miscible. The two components are partially miscible with each other in the expanded as well as in the condensed state.

On the other hand, the new finding is that FC16/DPPC two-component system has two regions; that is $\xi = -0.28$ for $X = 0$–0.3, and the collapse pressure is constant for $X < 0.3$–1. That is, they are miscible for $X = 0$–0.3. At the miscible region, the interaction parameter is $\xi = -0.28$. The negative interaction parameter implies that the interchange energy between different molecules is higher than the mean energy of interactions. Its interaction energy was calculated to be -116 J mol^{-1}. That is, they are miscible, because interaction energy ($-\Delta\varepsilon$) < $2RT$ (= 4958.7 J mol^{-1}). Two components are miscible each other in the expanded state and the condensed state for $X_{FC16} = 0$–0.3. For $X < 0.3$–1, FC16 and DPPC are completely phase-separated, which is assumed by fluorescence microscopy (later section).

The chain length of DPPC is shorter than that of FC18. The fluorocarbon part is more bulky than the hydrocarbon part at the air/water interface. As can be seen from Fig. 2, the π–A isotherms of FC18 are an ordered film type at 298.2 K. The FC18/DPPC binary system shows completely phase separation type, because two collapse pressures of individual pure components are seen over the whole mole fraction range (Fig. 3d) and also such behavior was assumed by fluorescence microscopy (later section).

3.4. Fluorescence microscopy of FC12/DPPC, FC14/DPPC, FC16/DPPC and FC18/DPPC

In order to interpret the phase behavior on the π–A isotherms, we investigated the monolayers by fluorescence microscopy, which provides a direct picture of the monolayers. A fluorescent dye probe was therefore incorporated into the monolayer and its distribution was determined by fluorescence micrographs. The contrast is due to difference in dye solubility between disordered (or LE) and ordered phases (or LC). Fluorescence micrographs (FMs) of pure DPPC and FC12, FC14, FC16 and FC18 monolayers spread at 298.2 K on 0.15 M NaCl (pH 2) are shown in Figs. 6 and 7 for various surface pressures. Image analysis was performed using NIH image. The percentage in FM images indicates parts of ordered (or LC) domain.

3.5. Fundamental shape characteristics of pure DPPC

Before examining the effects of a single chain fluorinated amphiphile on DPPC domain shape, a basic understanding of pure DPPC behavior is necessary. DPPC π–A isotherm is shown in Fig. 1, where there exists the LE/LC coexistence region. Domain nucleation occurs at the kink in the π–A isotherm (typically at 7.6 mN m^{-1}). Initially, the domains appear roughly round in shape: Whether the shape is the case in reality or due to limits in the resolution of the microscope is unclear. Indeed, only when they grow, they take their fundamental shape in Fig. 6a.

Fig. 6a shows a progression of fluorescence images through the coexistence region [56–58]. The surface pressures are noted in the figures. They indicate the gas phase

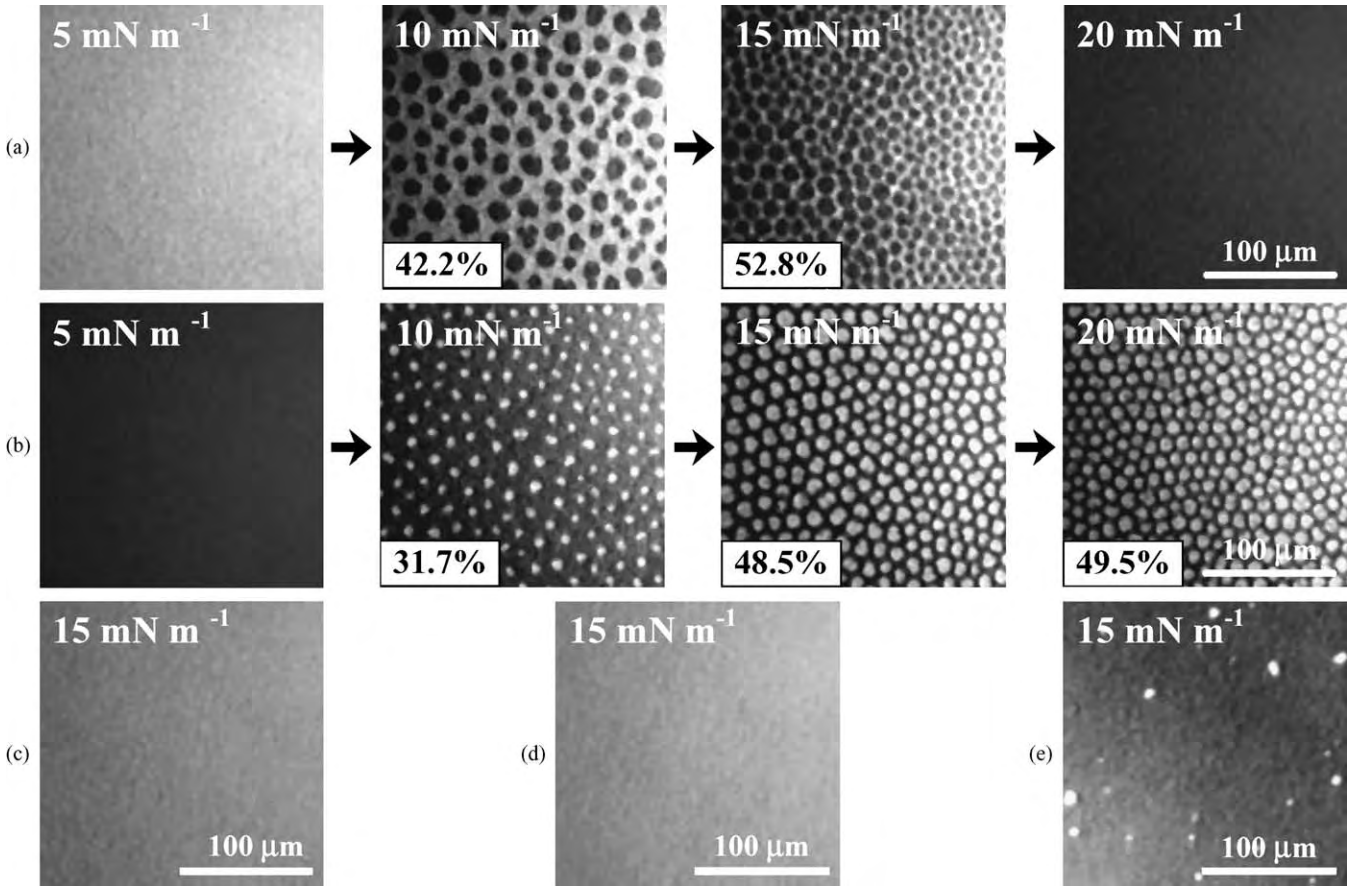

Fig. 6. Fluorescence micrographs of FC*n*s and DPPC at various surface pressures. In the coexistence states, the ratios of LC or ordered domains to the total micrographs are shown. The monolayers contain 1 mol% fluorescent probe (R18). The scale bar in the lower right represents 100 μm. (a) DPPC, (b) FC12, (c) FC14, (d) FC16 and (e) FC18. Percentage shows the ordered domain contents in the image.

at 5 mN m^{-1} and the coexistence state of LE phase and LC phase at 10 and 15 mN m^{-1}, where the bright regions and dark domains indicate LE and LC phase, respectively. With increasing surface pressure from 10 mN m^{-1} to 15 mN m^{-1}, the ratio of LC phase in each total image increases from 42.2% to 52.8% and only complete LC domain appears at 20 mN m^{-1}. The domains formed are chiral, which is an expression of the chirality of the DPPC molecule. As would be expected, the enantiomer forms mirror images of the domains, and a racemic mixture yields nonchiral domains. As is most evident in Fig. 6a at 10 mN m^{-1}, the predominant domain shape is a bean with distinct cavities. As the monolayer is compressed, the domains grow and display their repulsive nature (arising from their oriented dipoles) by deforming themselves to fill all available space and transforming into polygons. At the surface pressures between 11 mN m^{-1} and 15 mN m^{-1}, there happens a shape instability resulting in 'cutting' the domain along intrinsic chiral paths as shown in Fig. 6a at 15 mN m^{-1}. This phase transition is attributed to the presence of the fluorescence probe, because no such effect is seen by Brewster angle microscopy [57]. In addition, the phase transition is completely suppressed at higher compression rates, suggesting a kinetic rather than a thermodynamic origin.

3.6. Fundamental shape characteristics of pure FCn

The FC12 films (Fig. 6b) indicate the disordered phase at 5 mN m^{-1} and the coexistence of a disordered phase and ordered phase at 10–20 mN m^{-1}. In contrast with DPPC, the dark regions and bright domains indicate the ordered and disordered phase, respectively. With increasing surface pressure from 10 mN m^{-1} to 20 mN m^{-1}, the percentage of the ordered phase increases from 31.7 to 49.5 via 48.5%. The order phase is a LS phase, because a direct in situ investigation of the same monolayer via grazing incidence X-ray diffraction shows a single resolution-limited first-order peak at 1.25 Å^{-1} and a second-order peak at 2.16 Å^{-1} [59]. Such a picture is typical of a hexagonal lattice of closely packed upright molecules. At 4 °C the resolution-limited peak was observed from 5 nm^2 down to 0.3 nm^2. This fact shows the coexistence of an ordered phase and a gaseous phase. However, at 20 °C the resolution-limited peak of the ordered phase was not found above 0.80 nm^2, which is in excellent agreement

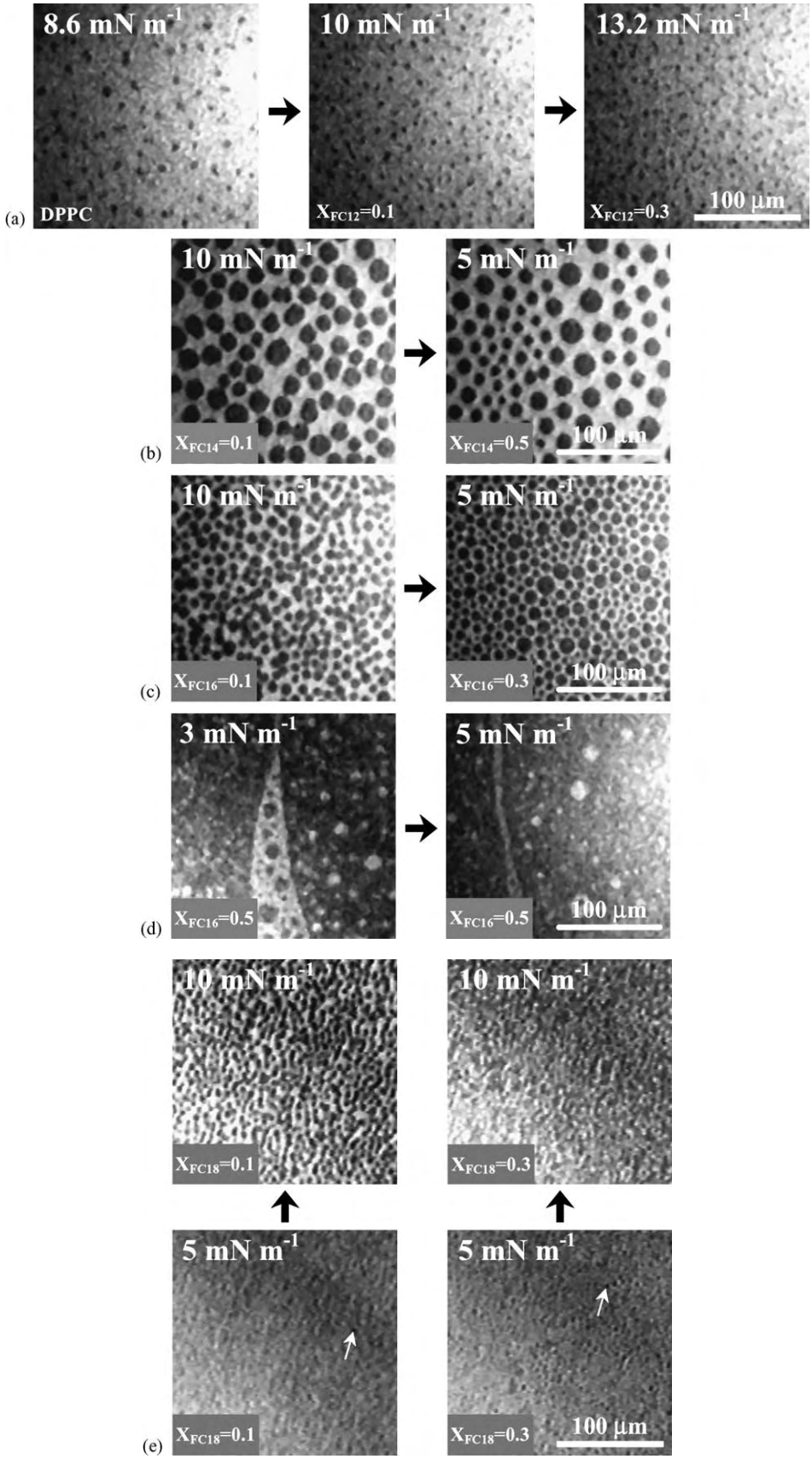

Fig. 7. Fluorescence micrographs of FC12/DPPC mixed monolayer (a), FC14/DPPC mixed monolayer (b), FC16/DPPC mixed monolayer (c, d) and FC18/DPPC mixed monolayer (e) observed on 0.15 M NaCl (pH 2) at 298.2 K. The monolayers contain 1 mol% fluorescent probe (R18). The scale bar in the lower left represents 100 μm.

with the above fluorescent microscopy data (Fig. 6b) and with the isotherm in Fig. 1. The structure found by the experimental study has also been confirmed via molecular dynamic simulation of the $CF_3(CF_2)_{13}COOH$ monolayer at 8 mN/m and 300 K by Shin and Rice [60]. Another theoretical paper by the same authors [61] explains the presence and the absence of tilting transition in monolayers for hydrocarbon and perfluorinated or nearly perfluorinated amphiphiles, respectively, via different amphiphile-amphiphile and amphiphile-water interactions at the surface. All the above investigations show that a first-order phase transition indeed exists in the uncharged perfluorinated monolayer, but it does occur between a disordered phase (gaseous or expanded) and an ordered (LS) one. So, in this FC12 too, the first-order transition is from L2 to LS.

In the case of FC14, FC16 and FC18 films (Fig. 2c–e), no change in image of fluorescent micrographs was observed. Especially in the FC18 films (Fig. 2e), there are many bright points which may be the appearance of the fluorescent probe. This indicates that FC18 and the fluorescent probe (R-18) are immiscible each other.

3.7. Two-component system

Next step, fluorescence measurement was done for two-component system, as shown in Fig. 7. It is clearly seen that comparing Fig. 7a–c, domain size is fixed in each case. In addition, the more increasing the mole fraction of FC12, the more increasing the transition pressure (π^{eq}) for the FC12/DPPC. On the contrary, increasing the mole fraction of FC*n* (*n* = 14 and 16), decreasing the transition pressure (π^{eq}) for the FC14/DPPC and FC16/DPPC on X_{FC16} = 0 ∼0.3. That is completely opposite direction. As long as we know, the new finding is that increasing the mole fraction of FC*n* results in decreasing the transition pressure (π^{eq}).

For FC16/DPPC on $X_{FC16} < 0.3$ and FC18/DPPC, the images of Fig. 7d and e do not change regardless of the incre-

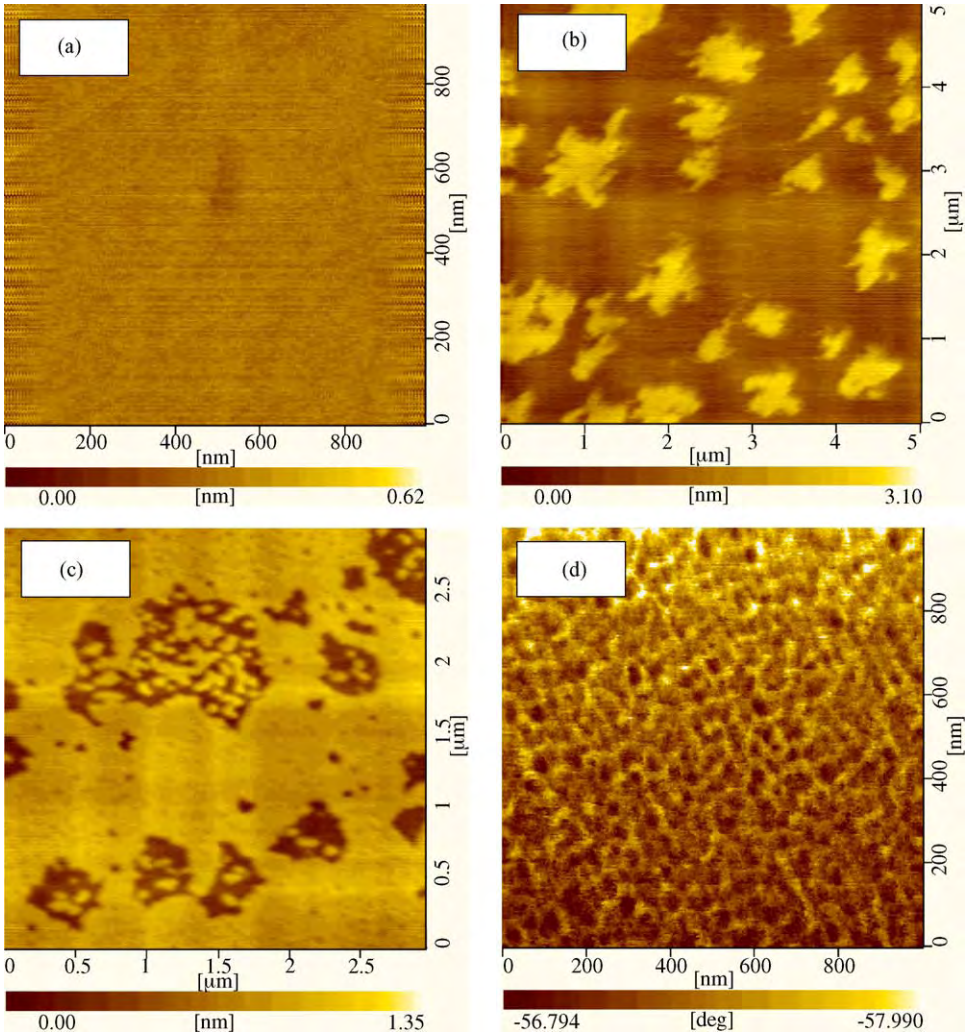

Fig. 8. AFM topography (a, b, c) and DFM topology (d) images on mica. The films were transferred to mica on 0.15 M NaCl (pH 2) at 20 mN m^{-1} and 298.2 K. (a) Pure DPPC monolayer (1 μm × 1 μm); (b) pure FC12 (5 μm × 5 μm); (c) X_{FC12} = 0.3 (3 μm × 3 μm); (d) X_{FC18} = 0.5 (1 μm × 1 μm).

ment of the mole fraction of perfluorocarboxylic acids. This pattern as was observed in Fig. 7d and e is considered to be a complete phase separation.

Judging from the appearance of coexistence regions in fluorescence images for each system, the two-dimensional phase diagrams of FC*n*/DPPC monolayers were constructed by plotting the values of transition pressure (π^{eq}) as a function of FC*n* mole fractions in Fig. 3. From the above results, perfluorinated amphiphiles have a drastic effect on the DPPC monolayer. Fluorescence microscopy on DPPC/FC12 shows that the perfluorinated amphiphiles dissolve the ordered solid DPPC domains that are formed upon compression. FC12 affects softening the lipid up to its specific mole fraction. On the other hand, FC14 and FC16 act to decrease the transition pressure. This indicates that these fluorinated amphiphiles dissolve the lipid by less amount. FC12 have a potential to soften the lipid more compared with FC14 and FC16.

3.7.1. AFM images of two-component systems

Langmuir–Blodgett (LB) films provide a model system of biological membrane. Atomic force microscopy (AFM) is a surface imaging technique with a nanometer-scale lateral resolution [62,63]. In comparison with the macro behavior of FC*n*s and DPPC system, the nanomorphological properties of FC*n*s/DPPC two-component systems deposited at a surface pressure of 20 mN m^{-1} were examined using AFM in order to clarify the miscibility between FC*n*s and DPPC in microphase scale (Fig. 8).

The DPPC showed an uniform pattern in the AFM image of Fig. 8a, while the FC12 showed an island pattern (b). This micrograph for pure FC12 (Fig. 8b) shows the coexistence state of ordered and disordered phases. That is, the bright island is the ordered domain of FC12 and dark pattern shows disordered domain. The difference in heights between the ordered domains the disordered domains was about 1.4 nm. The AFM image for the FC12/DPPC (X_{FC12} = 0.3) is shown in Fig. 8c. Small round-shape islands of the FC12 ordered domain were observed as the dark spots. The ordered domains of FC12 are dispersed in DPPC domains, indicating that FC12 and DPPC do not have a strong repulsion in micro scale. This pattern observed in Fig. 8c suggests that two components are completely miscible.

We had also measured DFM image for typical macro-immiscible system of FC18/DPPC (X_{FC18} = 0.5) which is shown in the topology of Fig. 8d. In this case, the chain lengths of perfluorinated chain and hydrocarbon are almost same and hence it is difficult to detect the difference between the perfluorinated chain and the hydrocarbon one by the topography of AFM and DFM. The phase contrast images were performed for the FC18/DPPC monolayers, as shown in Fig. 8d. The phase contrast image shows the stripe domains in several tens of nanometer-scale, and if two components are miscible, the image shows homogeneous. This immiscible pattern observed in Fig. 8d is considered to be a completely immiscible for FC18/DPPC monolayers in several tens of nanometer-scale.

The macro-properties of thermodynamic quantities and fluorescence microscopy observation correspond each other in a nanometer-scale.

4. Conclusion

The three types of phase diagrams were obtained and classified as follows: a positive azeotropic type, a partially positive azeotropic type and a completely immiscible one. Assuming a regular surface mixture, the Joos equation was applied to trace the collapse pressure of a two-component monolayer with miscible components. An interaction parameter (ξ) and interaction energy were calculated. The systems from phase diagrams and the two-component monolayer states at 298.2 K can be classified as 'Positive azeotropic system' (FC12/DPPC, FC14/DPPC): the two components are miscible with each other in the expanded as well as in the condensed state, where the mutual interaction between two components in the two-component monolayer is stronger than the mean of the interactions between pure component molecules themselves. The Joos equation allowed calculation of interaction parameter ($\xi = -0.58$) and the energy of interaction ($-\Delta\varepsilon$ = 240 J mol^{-1}) between FC12 and DPPC, and $\xi = -0.91$ and $-\Delta\varepsilon$ = 376 J mol^{-1} between FC14 and DPPC, respectively. 'Partially positive azeotropic type' (FC16/DPPC) consists of a combination of as 'positive azeotropic part' ($X_{FC16} < 0.3$) and complete phase separation part. Complete phase separation type shows two collapse pressures of individual pure components, which are seen over the region from 0.5 to 1 in mole fraction of FC16. The third case (FC18/DPPC) is completely immiscible. Complete phase separation type shows two collapse pressures of individual pure components as can be seen over the whole mole fraction region.

A new finding in the present study is that increasing the mole fraction of FC*n* results in decreasing the transition pressure (π^{eq}) for FC14/DPPC and FC16/DPPC two-component systems. This behavior is an evidence of the partial miscibility of the two components within the mixed monolayer. From the microscopic point of view, DPPC was compressed by extremely hydrophobic and lipophobic perfluorocarboxylic acids, and therefore, the resultant transition surface pressure was made of decrease depending on the mole fraction.

Fluorescence microscopy and atomic force microscopy (AFM) on FC*n*/DPPC and two-component monolayers on 0.15 M NaCl (pH 2) provide the information of a nanometer-scale. The macro properties of thermodynamic quantities and fluorescence microscopy observation are corresponded with each other in a nanometer-scale. Both results indicate that FC12 dissolves the ordered solid DPPC domains that are formed upon compression. On the other hand, FC14 and FC16 act to decrease the transition pressure. This in-

dicates that these fluorinated amphiphiles less dissolve the lipid. FC12 has a potential to soften the lipid more compared with FC14 and FC16, which indicates that FC12 liquified the lipid and that these materials will be useful to inform their innovative applications to the biomedical field.

Acknowledgements

This work was partially supported by Grant-in-Aid for Scientific Research from the Kieikai Foundation, which is greatly appreciated. Authors are indebted to Dr. V.Y. Shaovalov, Institute of Chemical Physics RAS, Russia, for the helpful advice of purification of perfluorocarboxylic acids (FC*n*s).

References

[1] M.P. Krafft, J.P. Rolland, P. Vierling, J.G. Riess, New J. Chem. 14 (1990) 869.
[2] M.P. Krafft, P. Vierling, J.G. Riess, Eur. J. Med. Chem. 26 (1991) 545.
[3] M.P. Krafft, J.G. Riess, Biochimie 80 (1998) 489.
[4] J.G. Riess, M.P. Krafft, Biomaterials 19 (1998) 1529.
[5] J.G. Riess, Tetrahedron 58 (2002) 4113.
[6] J.G. Riess, Chem. Rev. 101 (2001) 2797.
[7] E.G. Schutt, D.H. Klein, R.M. Mattrey, J.G. Riess, Angew. Chem. Int. Ed. Engl. 42 (2003) 3218.
[8] J.G. Riess, New J. Chem. 19 (1995) 893;
J.G. Riess, in: T.M.S. Chang, J.G. Riess, R.M. Winslow (Eds.), Proceedings of the 5th International Symposium on Blood Substitutes, San Diego, CA, March 1993, Art. Cells Blood Subst. Immob. Biotechnol. 1 (1994);
J.G. Riess (Ed.), Blood Substitutes and Related Products. The Fluorocarbon Approach.
[9] (a) J.G. Riess, J. Drug Target. 2 (1994) 455;
(b) J.G. Riess, M.P. Krafft, Chem. Phys. Lipids 75 (1995) 1;
(c) J.G. Riess, J. Liposome Res. 5 (1995) 413;
(d) J.G. Riess, F. Frezard, J. Greiner, M.P. Krafft, C. Santaella, P. Vierling, L. Zarif, in: Y. Barenholz, D. Lasic (Eds.), Liposomes-Nonmedical Applications, vol.111, CRC Press, Boca Raton, FL, 1996, p. 97.
[10] V.M. Sadtler, M.P. Krafft, J.G. Riess, Angew. Chem., Int. Ed. Engl. 35 (1996) 1976.
[11] M.P. Krafft, J.G. Riess, J.G. Weers, in: S. Benita (Ed.), Submicronic Emulsions in Drug Targeting and Delivery, Harwood Academic Publication, Amsterdam, 1998, p. 235.
[12] M.P. Krafft, Adv. Drug Deliv. Rev. 47 (2001) 209.
[13] N.K. Adam, The Physics and Chemistry of Surfaces, Dover publications Inc., 1968 (Chapter 2).
[14] W.D. Harkins, The Physical Chemistry of Surface Films, Reinhold Publishing Co., New York, 1952 (Chapter 2).
[15] G.L. Gaines, Insoluble Monolayers at Liquid–Gas Interfaces, Interscience Publishers, 1966.
[16] (a) H. Matuo, N. Yoshida, K. Motomura, R. Matuura, Bull. Chem. Soc. Jpn. 52 (1979) 667;
(b) H. Matuo, K. Motomura, R. Matuura, Bull. Chem. Soc. Jpn. 52 (1979) 673, and 54 (1981) 2205;
(c) H. Matuo, K. Motomura, R. Matuura, Chem. Phys. Lipids 28 (1981) 281/385, and 30 (1982) 353;
(d) H. Matuo, D.K. Rice, D.M. Balthasar, D.A. Cadenhead, Chem. Phys. Lipids 30 (1982) 367;
(e) H. Matuo, T. Mitsui, K. Motomura, R. Matuura, Chem. Phys. Lipids 29 (1981) 55.
[17] H.-J. Lehmler, M. Jay, P.M. Bummer, Langmuir 16 (2000) 10161.
[18] H.-J. Lehmler, M.O. Oyewumi, M. Jay, P.M. Bummer, J. Fluor. Chem. 107 (2001) 141.
[19] H.-J. Lehmler, P.M. Bummer, J. Colloid Interface Sci. 249 (2002) 381.
[20] M. Arora, P.M. Bummer, H.-J. Lehmler, Langmuir 19 (2003) 8843.
[21] S. Yamamoto, O. Shibata, S. Lee, G. Sugihara, Prog. Aneth. Mech. 3 (Special Issue) (1995) 25.
[22] O. Shibata, M.P. Krafft, Langmuir 16 (2000) 10281.
[23] H.M. Courrier, T.F. Vandamme, M.P. Krafft, S. Nakamura, O. Shibata, Colloids Surf. A 33 (2003) 215.
[24] T. Hiranita, S. Nakamura, M. Kawachi, H.M. Courrier, T.F. Vandamme, M.P. Krafft, O. Shibata, J. Colloid Interface Sci. 265 (2003) 83.
[25] H. Kawasaki, M. Syuto, H. Maeda, Langmuir 17 (2001) 8210.
[26] M. Takizawa, Y.H. Kim, T. Urisy, Chem. Phys. Lett. 385 (2004) 220.
[27] M. Rusdi, Y. Moroi, S. Nakamura, O. Shibata, Y. Abe, T. Takahashi, J. Colloid Interface Sci. 243 (2001) 370.
[28] T. Kato, M. Kameyama, M. Ehara, K.-I. Iimura, Langmuir 14 (1998) 1786.
[29] H. Morgan, D.M. Taylor, O.N. Oliveira Jr., Biochim. Biophys. Acta 1062 (1991) 149.
[30] V.L. Shapovalov, Thin Solid Films 327/329 (1998) 599.
[31] D. Honig, D. Möbius, Thin Solid Films 210–211 (1992) 64.
[32] H.W. Fox, J. Phys. Chem. 61 (1957) 1058.
[33] M.K. Bernett, W.A. Zisman, J. Phys. Chem. 67 (1963) 1534.
[34] M.K. Bernett, N.L. Jarvis, W.A. Zisman, J. Phys. Chem. 68 (1964) 3520.
[35] V. Vogel, D. Möbius, Thin Solid Films 159 (1988) 73.
[36] D. Ducharme, C. Salesse, R.M. Leblanc, Thin Solid Films 132 (1985) 83.
[37] O.N. Oliveira Jr., A. Cavalli, J. Phys.: Condens. Matter 5 (1993) 307.
[38] O.N. Oliveira Jr., C. Bonardi, Langmuir 13 (1997) 5920.
[39] P. Luckham, J. Wood, S. Froggat, R. Swart, J. Colloid Interface Sci. 156 (1993) 164.
[40] E. Dupart, B. Agricole, S. Ravaine, C. Mingotaud, O. Fichet, P. Delhaes, H. Ohnuki, G. Munger, R.M. Leblanc, Thin Solid Films 243 (1994) 575.
[41] O. Befort, D. Möbius, Thin Solid Films 243 (1994) 553.
[42] T. Kondo, R.C. Ahuja, D. Möbius, M. Fujihira, Bull. Chem. Soc. Jpn. 67 (1994) 315.
[43] R.C. Ahuja, P. Caruso, D. Möbius, G. Wildburg, H. Ringsdorf, D. Philip, J.A. Preece, J.F. Stoddart, Langmuir 9 (1993) 1534.
[44] K. Ohara, M. Nakajima, Thin Solid Films 226 (1993) 164.
[45] O. Fichet, D. Ducharme, V. Gions, P. Delhaes, R.M. Leblanc, Langmuir 9 (1993) 491.
[46] D.M. Taylor, O.N. Oliveira Jr., H. Morgan, Thin Solid Films 173 (1989) 141.
[47] A. Sugimura, M. Iwamoto, O.Y. Zhong-can, Phys. Rev. E 50 (1995) 614.
[48] M. Iwamoto, T. Kubota, M.R. Muhamad, J. Chem. Phys. 102 (1995) 9368.
[49] M. Iwamoto, Y. Mizutani, Phys. Rev. B 54 (1996) 8186.
[50] (a) J. Marsden, J.H. Schulman, Trans. Faraday Soc. 34 (1938) 748;
(b) D.O. Shah, J.H. Schulman, J. Lipid Res. 8 (1967) 215.
[51] C.A. Helm, H. Möhwald, K. Kjaer, J. Als-Nielsen, Biophys. J. 52 (1987) 381.
[52] O. Albrecht, H. Gruler, E. Sackmann, J. Phys. (France) 39 (1978) 301.

[53] V.M. Kaganer, H. Möhwald, P. Dutta, Rev. Mod. Phys. 71 (1999) 779.
[54] Y.K. Levine, Prog. Surf. Sci. 3 (1973) 279.
[55] P. Joos, R.A. Demel, Biochim. Biophys. Acta 183 (1969) 447.
[56] C.W. McConlogue, T.K. Vanderlick, Langmuir 13 (1997) 7158.
[57] C.W. McConlogue, T.K. Vanderlick, Langmuir 14 (1998) 6556.
[58] C.W. McConlogue, D. Malamud, T.K. Vanderlick, Biochim. Biophys. Acta 1372 (1998) 124.
[59] A.A. Acero, M. Li, B. Lin, S.A. Rice, M. Goldmann, I.B. Azouz, A. Goudot, F. Rondelez, J. Chem. Phys. 99 (9) (1993) 7214.
[60] S. Shin, S.A. Rice, Langmuir 10 (1994) 262.
[61] S. Shin, S.A. Rice, J. Chem. Phys. 101 (3) (1994) 2508.
[62] T. Kato, N. Matsumoto, M. Kawano, N. Suzuki, T. Araki, K. Iriyama, Thin Solid Films 242 (1994) 223.
[63] E. Meyer, R. Overney, R. Lüthi, D. Brodbeck, L. Howald, J. Frommer, H.-J. Güntherodt, O. Wolter, M. Fujihira, H. Takano, Y. Gotoh, Thin Solid Films 220 (1992) 132.